WPDIV-CPR(17) 17054

F Gallay et al.

Infrared thermography inspection of novel divertor target components for DEMO

Preprint of Paper to be submitted for publication in Proceeding of 16th International Conference on Plasma-Facing Materials and Components for Fusion Applications

This work has been carried out within the framework of the EUROfusion Consortium and has received funding from the Euratom research and training programme 2014-2018 under grant agreement No 633053. The views and opinions expressed herein do not necessarily reflect those of the European Commission.

Quantitative thermal imperfection definition using non-destructive infrared thermography on an advanced DEMO divertor concept

F. Gallay[a,*], M.Richou[a], N. Vignal[a], M. Lenci[b], S. Roccella[c], G. Kermouche[b], E. Visca[c], and J.H. You[d],

[a] *CEA, IRFM, F-13108 Saint-Paul-Lez-Durance, France*

[b] *École nationale supérieure des mines de Saint-Étienne, Centre SMS CNRS UMR 5307 Laboratoire Georges FRIEDEL,158 cours Fauriel, CS 62362*

[c] *ENEA, Unità Tecnica Fusione, ENEA C. R. Frascati, via E. Fermi 45, 00044 Frascati, Italy*

[d] *Max Planck Institute for Plasma Physics, Boltzmann Str. 2, 85748 Garching, Germany*

For the DEMO power reactor, conceptual representative components of the divertor are currently developed and qualified with the manufacturing of various mock-ups. These plasma-facing-components will need a large power exhaust capability and must withstand high constraints (up to 20 MW/m² during slow transient events). In order to guarantee the integrity of these mock-ups, their thermal and mechanical behaviour must be assessed preliminary. The examination of the heatsink to armor joints with non-destructive techniques is an essential topic to be addressed. This paper reports about the thermal imperfection detection using infrared thermography examination (using SATIR test facility) of mock-ups equipped with graded material as interlayer. In order to precise the origin, the position, the size and the criticality of such imperfection, correlations of SATIR tests, finite element method modeling and other techniques (ultrasonic testing, metallographic examinations) are performed and reported. Results, using a new developed method, show an improvement in thermal imperfection extension assessment.

Keywords: DEMO, Divertor, Infrared thermography, non-destructive examination, Plasma-facing component

1. Introduction

In the framework of the EUROfusion Consortium, a program of conceptual design activities for the European DEMO reactor [1] has been launched in 2014. One of the plasma-facing components (PFCs) concerned by these activities is the DEMO divertor target which will have to withstand high thermal loads (up to 20 MW/m² during slow transient events). In order to fulfil the relevant structural design criteria in such a harsh loading environment, novel design concepts are currently under development and are being qualified with the manufacturing of various mock-ups [2]. In order to ensure the integrity of these mock-ups, their thermal and mechanical behaviours should be assessed in advance. Major risks of the presence of thermal imperfections in PFCs are that the heat loads can induce debonding between armor and structural material or induce cracks. The non-destructive examination [3] using SATIR facility (French acronym for the IR acquisition and data processing device) has proven to be a relevant technique to detect such imperfections [4-6]. Within WP-DIV project, mock-ups of different design concepts have been tested using SATIR test bench before high-heat-flux testing. Results of SATIR tests showed acceptable thermal exhaust capabilities for more than 94% of the tested components [7]. However, some monoblocks present abnormal thermal behaviours and delays in reaching thermal equilibrium compared to the reference monoblocks. Precise identification of the origin, position, size and the impact of these thermal perturbations can help to define acceptance of PFCs [4]. With SATIR test data, a first method to assess imperfection size and position for monoblock concepts was developed [5] and is applied. Nevertheless, this method requires (for each tested concept) a calibration with manufactured artificial defects [4-6]. Therefore, because of the various geometries proposed in WP-DIV project and to avoid these expensive fabrications a second method is investigated here by comparing numerical simulations and experimental data of SATIR test. Both thermal imperfection characterization methods are applied for one design concept using graded interlayer (developed by CEA) [7] and correlated with those of other complementary test techniques such as metallographic examinations and ultrasonic tests [8].

2. Mock-ups description

For DEMO divertor, the envisaged armor material is tungsten. As baseline structural materials copper alloy CuCrZr has been chosen due to its important thermal conductivity and mechanical properties at foreseen operation temperature (150 °C to 350 °C) [9].

Various kinds of novel interlayer materials are envisaged to replace CuOFHC used in ITER divertor concept as a compliant layer between W and CuCrZr [2]. One of these concepts, which is studied here, uses Functionally Graded Material (FGM) as an interlayer [7]. For this concept, the Cu alloy cooling tube was joined using a very thin graded W/Cu film as bonding agent without thick Cu interlayer. The mock-ups consist of 10 tungsten monoblocks (size 4 mm x 22 mm x 23 mm) with an adhesive deposit of FGM at internal part (thickness ~25 µm) and assembled with a CuCrZr tube. Schematic view of geometry is shown in Fig.1.

Seven mock-ups of this concept have been manufactured (mock-up M0 to M6) and qualified by SATIR, Ultrasonic tests (UT), and high heat flux tests [7].

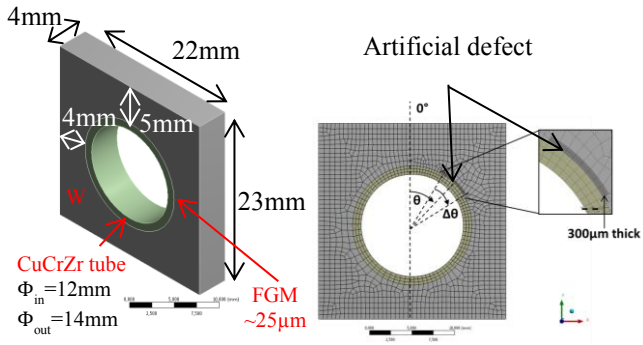

Fig. 1 Sketch of monoblock geometries with (right) and without (left) thermal imperfection

3. Defect detection methods

3.1 SATIR

SATIR facility is an active Infrared thermography test bed based on the heat transient method [10]. Developed at CEA this installation is able to determine heat exhaust capability of components and to detect potential thermal imperfections in PFCs. This technique is based on thermal inspection of the component during a fast temperature variation (105–10 °C in few ms) of water flowing in the cooling channel of a target mock-up. The surface temperature is measured during the transient phase via an IR camera (CEDIP JADE II λ=3-5 µm). In this test, the transient evolution of surface temperature of the examined mock-up is compared with that of a reference mock-up being defect-free. The maximum temperature difference for each pixel (DtRef) occurring during the cooling transient is analyzed. For each examined face of the component, coresponding DtRef maps are extracted and $DtRef_{max}$ is calculated and corresponds to the maximum of all DtRef values. A slower surface temperature response, monitored by infrared camera is interpreted as a higher thermal resistance, i.e. bad joining between different layers of materials or defects in materials.

3.2 Method 1: EQuivalent thermal Imperfection (EQI)

To assess thermal imperfection size and position, a first method relies on implementation of an EQI threshold on DtRef values [5]. DtRef values higher than EQI threshold may be attributed to the presence of thermal imperfection located on the thermal path from the cooling tube to the observed external surface. These thermal imperfections are most likely due to interlayer/CuCrZr interface debonding [11]. Consequently, DtRef maps are attributed to an EQI at the surface of the external CuCrZr tube. It is described as an extension (Δθ) and position (θ) of probable thermal imperfection. For this EQI definition, 2D DtRef maps of all faces are geometrically projected onto the external CuCrZr tube map and EQI threshold is applied [5].

One limit of EQI method is that, for each tested geometry, EQI threshold must be assessed preliminary with dedicated calibration and examination of manufactured artificial calibrated defects [4-6]. With the several geometries developed in WPDIV project, and thereby the many artificial defects to manufacture (at least two or three by concept), this calibration appears complex to achieve. For this reason, and based on a past experience [6], EQI threshold is here set to the value of 8°C without performing any calibration.

3.3 Method 2: FEM modeled Imperfection (FEMI)

Another approach, FEMI method, consists in comparing finite element method (FEM) modeling with SATIR experimental results. The most important benefit compared to EQI method is that FEMI method is not linked to an EQI threshold.

Nevertheless, as a preliminary study, and for comparison purpose, thermal imperfection position (θ) and extension (Δθ) are only assessed for monoblocks with DtRef values higher than EQI threshold (i.e: 8°C).

For SATIR experimental data extraction, 2D DtRef maps of all faces are firstly geometrically projected onto the external CuCrZr tube map. Then, for the purpose of the analysis, experimental 1D DtRef profile is extracted at the monoblock depth including $DtRef_{max}$.

For modeled data extraction, SATIR experiments of a defective monoblock and a defect-free monoblock are simulated using 2D FEM modeling with ANSYS V17.2. Implemented geometries with and without defect are presented in Fig. 1. The thin FGM thickness of ~25 µm has been neglected due to its negligible effect on the surface temperature behavior. For defective monoblock geometries, artificial defects implemented have a thickness of 300 µm (see Fig. 1) with air thermal properties. The choice of modeling standardized imperfection (~300 µm) at W to bond-layer has been made since imperfections are most likely of this thickness and frequently positioned at this interface [4]. In the following, such defect will be called standard defect. Thermal conductivities and convection coefficient in the inner tube have been implemented at representative temperature evolution of SATIR test. Radiation and convection on external surfaces with ambient have been neglected. Surface temperature for each node is obtained for geometries with and without thermal imperfection. The maximum temperature difference between those two geometries and for each node occurring during the cooling transient of the W surface is calculated and projected at the CuCrZr/interlayer interface allowing to define modeled 1D DtRef profiles.

Since differences exist between experimental and numerical $DtRef_{max}$ data [6], experimental and modeled 1D DtRef profiles are normalized.

Finally, FEMI position (θ) is assessed at the angle corresponding to the peak value of experimental 1D DtRef profiles. FEMI extension (Δθ) corresponds to the artificial defect extension Δθ for which modelled 1D

DtRef profile show most-fitted curve shape with experimental 1D DtRef profile.

4. Experimental results

To evaluate EQI & FEMI methods, results for two monoblocks of mock-up M0 are firstly presented and correlated with metallographic examinations. Afterwards, these methods are applied to other mock-ups (M1 to M6) and correlated with ultrasonic tests results as for these mock-ups no metallographic examinations were performed.

4.1 EQuivalent thermal Imperfection (EQI) results

With EQI method applied to mock-up M0, two monoblocks are evaluated as presenting some thermal imperfections: M0-1, with a thermal imperfection of extension $\Delta\theta$=80° and positioned at θ=35° and M0-9, with a thermal imperfection of extension $\Delta\theta$=20° and positioned at θ=-105°. Corresponding results are summarized in Table 1.

4.2 FEM modeled Imperfection (FEMI) results

For M0-1 and M0-9, experimental 1D DtRef profiles and corresponding peak value positions show (see Fig. 2) imperfections positioned at respectively θ= 50° and θ= -110°.

For both monoblocks, modeled 1D DtRef profiles show symmetrical curve shapes centered (see Fig. 2) on θ. For M0-9, and for a wide range of angles around θ [-180°; 50°], a good agreement between modeled and experimental profiles is observed. For M0-1 though, an asymmetrical experimental curve shape is observed and therefore a restricted area is arbitrary selected and aimed to fit with modeled data namely [θ= 50°; 180°]. The modeled curve shape fit only in this restrictive area with the experimental profile. The asymmetry of experimental profile and the difficulty to fit profiles might be explained by differences between modeled and real defect in terms of defect shape, thickness or radial position. For this reason, when experimental and modeled profiles don't fit, non-standard defect can be foreseen.

Finally, extensions of $\Delta\theta$ =270° for M0-1 and of $\Delta\theta$ =95° for M0-9 are assessed (Table 1).

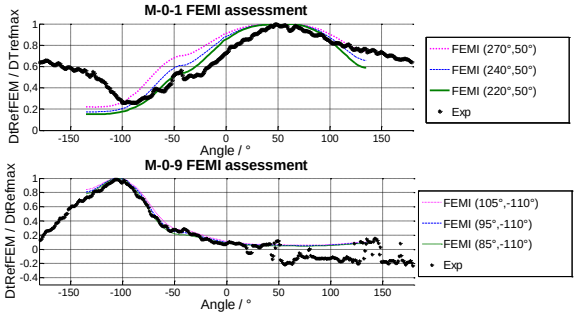

Fig. 2 Correlations of experimental and modeled profiles

4.3 Definition of the thermal imperfection reference size

Definition of the thermal imperfection reference size is performed using different techniques (Visual observation after metallographic examination for M0 and ultrasonic testing for M1 to M6).

For Mock-up M0, monoblocks M0-1 and M0-9 were cut and examined with an optical microscope (Olympus BX60M) and a binocular magnifier (Olympus SZX9).

With these metallographic observations two kinds of damages are highlighted. For M0-1, a thin crack propagating circumferentially, at a distance of 1.5 mm with an extension of $\Delta\theta$ =300° and positioned at θ =70° is detected. For M0-9, cavities (size ~500µm) and cracks are emphasized, at a distance <200µm with a total extension of $\Delta\theta$= 105°. Imperfection is consequently centered and positioned at θ=-117° (see Fig. 3).

Mock-ups M1 to M6 were examined with ultrasonic testing [8] which is assumed to be, for these mock-ups, the reference for the size determination of thermal imperfection.

Results of both technics are summarized in Table 1.

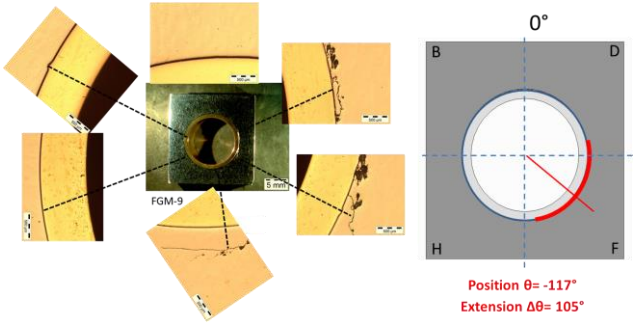

Fig. 3: Metallographic observation of monoblock M0-9

4.4 Evaluation of EQI and FEMI methods

In this part, positions and extensions of thermal imperfections are assessed for all tested mock-ups (see Table 1). Results are compared with the thermal imperfection reference size defined in the previous paragraph.

For mock-up M0, comparisons of metallographic observations with EQI results (see Table 1) show significant underestimations of the thermal imperfection extensions (-81% for M0-9). These errors show that applying EQI method with arbitrary threshold may generate important errors on the thermal imperfection size definitions.

For M0-1, FEMI method data processing shows that modeled data are difficult to fit with experimental data. Consequently, a non-standard defect is foreseen and finally confirmed by metallographic examination. Despite this, the error compared to metallographic examination is reduced to 10%.

For M0-9, FEMI method result shows a good agreement with metallographic observations and reduced error compared to EQI method result.

For M2-1, both methods show consistent results with UT examination with an extension of $\Delta\theta$ = 360°.

For M2-10, FEMI method result shows an improvement of extension assessment precision compared to EQI method.
Finally, for M6-10 FEMI method result retains an important error of 22%. For this monoblock, data processing also shows important differences between modeled and experimental data which may be explained by the fact that defect is localised in tungsten [7] but modeled at interface.
To conclude, for the tested components, FEMI method allows assessing precisely (with a precision of ~9%) thermal imperfection extension when thermal imperfection is positioned at the interface. Otherwise, it was observed in this study that for all modeled thermal imperfection, if experimental and modeled profiles don't succeed to fit, errors (up to -22%) can be observed and may be explained by the fact that defect were not modeled representatively as the real defect. Consequently, with FEMI method, the presence of non-standard defects can be foreseen and eventually confirmed with achieving further tests such as ultrasonic testing in the whole monoblock thickness (and not only at interface).
One prospect is to apply FEMI method to all monoblocks presenting DtRef experimental profiles typical of monoblock with thermal imperfection (i.e: Gaussian).

Monoblock	EQI (Δθ,θ)	Error (%)	FEMI (Δθ,θ)	Error (%)	Ref. (Δθ,θ)
M0-1	80°,35°	-70%	270°,50°	-10%	300°,70*****
M0-9	20°,-105°	-81%	95°,-110°	-9%	105°,-117°
M2-1	360°	0%	360°	0%	360°
M2-10	300°,140°	10%	280°,140°	3%	270°,145°
M6-10	135°,70°	-22%	135,70°	-22%	173°,65°*****

Table 1 EQI/ FEMI thermal imperfections assessments and errors in comparison with reference (i.e: metallographic examinations for Mock-up M0, Ultrasonic Testing (UT) for other mock-ups) (***** defect detected in the bulk tungsten)

5. Conclusion

Infrared thermography using SATIR facility allows assessing heat exhaust capability of plasma facing components which may be weaken by the presence of thermal imperfection at material interfaces. For that reason, the quantification of thermal imperfection position, size and origin with the use of non-destructive technics is an important topic to be addressed. In this work, the reliability of SATIR tests coupled to one existing (EQI) method to assess quantitatively thermal imperfection size and position has been evaluated. It was observed that this method can present some significant inaccuracies for the extension determination (errors up to -81%). In order to reduce these errors and to avoid costly calibration, a development of a new method, based on correlations between modeling and SATIR experimental results, has been performed and shows improvement of up to 59% in thermal imperfection extension assessment. This new (FEMI) method doesn't require manufacturing process nor threshold determination and could potentially be applied for any kind of geometry and known material.
To conclude, SATIR coupled to FEMI method appear to be relevant to detect and characterize thermal imperfection with an accuracy of ~9% for the analyzed monoblocks and when thermal imperfection are positioned at the interface. When important differences between experimental and simulated DtRef data are observed, thermal imperfection may be different from the one which is modeled in terms of shape, thickness or location in the monoblock. In this case additional non-destructive examination such as Ultrasonic Tests and data merging [12] could also be used.

Acknowledgments

This work has been carried out within the framework of the EUROfusion Consortium and has received funding from the Euratom research and training programme 2014-2018 under grant agreement No 633053. The views and opinions expressed herein do not necessarily reflect those of the European Commission

References

[1] You J H *et al* 2016 *Nuclear materials and Energy* **9** 171
[2] You J H *et al* 2016 *Fusion Eng. Des.* **109** 1598
[3] Merola M *et al* 2002 *Fusion Eng. Des.* **61** 141
[4] Escourbiac F, Richou M, Guigon R, Constans S, Durocher A, Merola M, Schlosser J, Riccardi B and Grosman A 2009 *Physica Scripta* **2009** T138
[5] Durocher A, Escourbiac F, Richou M, Vignal N, Merola M, Riccardi B, Cantone V and Constans S 2009 *Fusion Eng. Des.* **84** 314
[6] Richou M, Escourbiac F, Missirlian M, Vignal N, Cantone V and Riccardi B 2011 *J. Nucl. Mater.* **417** 581
[7] Richou M, Gallay F, Chu I, Li M, Magaud P, Missirlian M, Rocella S, Visca E and You J H 2017 *Fusion Eng. Des.* At press
[8] Roccella S, Cacciotti E, Escourbiac F, Pizzuto A, Riccardi B, Tatì A, Varone P and Visca E 2009 *Fusion Eng. Des.* **84** 1639
[9] Li Puma A, Richou M, Magaud P, Missirlian M, Visca E and Ridolfini V P 2013 *Fusion Eng. Des.* **88** 1836
[10] Vignal N, Desgranges C, Cantone V, Richou M, Courtois X, Missirlian M and Magaud P 2013 *Fusion Eng. Des.* **88** 1818
[11] Richou M, Missirlian M, Vignal N, Cantone V, Hernandez C, Norajitra P and Spatafora L 2013 *Fusion Eng. Des.* **88** 1753
[12] Richou M, Durocher A, Medrano M, Martinez-Oña R, Moysan J and Riccardi B 2009 *Fusion Eng. Des.* **84** 1593